Influence of Impulse Noise on Alamouti Code Performances

Mihaela Andrei, Lucian Trifina, and Daniela Tarniceriu

Abstract. Multiple-Input Multiple-Output systems ensure spatial diversity and fading protection for wireless communications. This paper addresses the impulse noise described by the Middleton Class-A statistical model, which can affect their performances. We have analyzed the influence of impulse noise, described by Middleton Class-A non-Gaussian model on the performances of the Alamouti code, with two transmitting antennas and two receiving antennas, on channels affected by Rayleigh fading, with Binary Phase-Shift Keying modulation. The simulations were made for different parameter values of the noise model and they showed that as the Signal-to-Noise Ratio increases, the performances decrease for the impulse noise compared with the Gaussian one. It is shown that BPSK modulation is more robust than QPSK one, used in transmission over impulse noise environment using an Alamouti code.

1 Introduction

Optimizing wireless communications entails the possibility of transmitting a large amount of information in a very short period of time and with as few errors as possible. A factor that influences significantly the communication quality is the propagation environment. This can lead to either attenuation of the received signal, known as *fading*, or introduction of certain delays, or phase shifting for one or more frequency components. All of these lead to the receiver's inability to recover the signal. The solution for this problem is to transmit more signal replicas, a technique known as *diversity* (spatial, temporal or frequency). [1]

Mihaela Andrei
Department of Electronics & Telecommunications,
"Dunarea de Jos" University of Galati, Romania
e-mail: mihaela.andrei@ugal.ro

Lucian Trifina · Daniela Tarniceriu
Department of Telecommunications,
"Gheorghe Asachi" Technical University Iasi, Romania
e-mail: {luciant,tarniced}@etti.tuiasi.ro

L. De Strycker (ed.), *ECUMICT 2014*,
Lecture Notes in Electrical Engineering 302,
DOI: 10.1007/978-3-319-05440-7_2, © Springer International Publishing Switzerland 2014

The systems that provide spatial diversity and successfully repel the fading are the Multiple-Input Multiple-Output (MIMO) ones. They involve multiple antennas for both transmission and reception. Among the encoding techniques used for the above-mentioned channels, a special interest is given to space-time codes (block, trellis or Bell labs LAyered Space-Time - BLAST), because they improve the data transmission safety, especially at high speeds [2].

The signals are not affected only by fading, but also by noise. For the majority of the proposed codes, the channel affected by fading and Gaussian white noise (AWGN) was considered, ignoring other sources of noise, like: industrial noise, man-made activity such as automobile spark plugs [3], microwave ovens [4] and network interference [5], noises known to be non-Gaussian.

So, we need to perform an analysis of communication systems in the presence of impulse noise (non-Gaussian) and, obviously, to try to eliminate or at least diminish its disruptive effects. The Middleton Class-A model is frequently used for modeling the impulse noise.

This type of noise has been used for investigating the performances of the orthogonal space-time codes (OSTBC), for QPSK and 16QAM modulations, respectively, on MIMO channels affected by Rayleigh fading [6] by comparing the Symbol Error Rate (SER) curves with the ones obtained when only the Gaussian noise was present. By varying the parameters that describe the noise model, for low values of Signal-to-Noise Ratio (SNR), the coding gain drops with at most 6dB compared to the Gaussian model, after which, along with the SNR increases, the system's performance drops in the case of non-Gaussian noise.

Most of the systems affected by non-Gaussian noise suffer performance degradation for high SNR values [7]. For example, in [8] an increase of the Bit Error Rate (BER) is observed for IEEE 802.11a and IEEE 802.11b, under the influence of Middleton Class-A noise compared to AWGN.

This paper proposes an analysis of the non-Gaussian noise, expressed through the Middleton Class-A statistical model. It investigates the OSTBC Alamouti code performances, on channels affected by Rayleigh fading, with BPSK modulation, and maximum likelihood (ML) receiver, with non-Gaussian and AWGN, respectively. Several parameters modeling the non-Gaussian noise were considered.

The paper is structured as follows. Sect. 2 describes the Middleton Class-A impulse noise model and Sect. 3 presents the system model. The simulation results are shown in Sect. 4 and conclusions are highlighted in Sect. 5.

2 Middleton Class-A Model

The non-Gaussian noise has a Gaussian component (n_g), with variance σ_g^2, and an impulse one (n_i), with variance σ_i^2. Thereby, the model for non-Gaussian noise can be considered as Additive White Class A Noise (AWCN):

$$n = n_g + n_i , \tag{1}$$

whose probability density function follows a Middleton Class-A distribution [6]. Its expression, for complex noise, is given by:

$$p(n) = \sum_{m=0}^{\infty} \frac{A^m e^{-A}}{\pi m! \sigma_m^2} exp\left(-\frac{|n|^2}{\sigma_m^2} \right) \tag{2}$$

We can observe that this is a Poisson weighted sum of Gaussian distributions. In (2), the terms have the following meaning: m is the number of active interferences (or impulses), and A is the impulse index and indicates the average number of impulses during interference time. This parameter allows the description of noise as follows: as A gets smaller, the noise gets more impulsive; conversely, as A grows, the noise tends towards AWGN.

σ_m^2 represents the noise's total variance and it is given by:

$$\sigma_m^2 = \frac{\frac{m}{A} + T}{1 + T} , \tag{3}$$

where

$$T = \frac{\sigma_g^2}{\sigma_i^2} \tag{4}$$

is called Gaussian factor. From its expression, we can observe that, for low T values, the impulsive component dominates, and for large T values, the AWGN component is the one that prevails.

3 Mathematical Model of MIMO System

MIMO communication channels involve multiple antennas for both transmission and reception, this way achieving spatial diversity. In this paper we assume that the propagation channels are without memory and they are affected by flat fading (Rayleigh type). Let there be a system with N_T emitting and N_R receiving antennas.

During one symbol, the transmitted signals x_i, form a column array, denoted by **x**, of size $[N_T, 1]$:

$$\mathbf{x} = \left[x_1, x_2 \ \ldots \ x_{N_T} \right]^T, \tag{5}$$

where i represents the index of the emitting antenna.

The linear input-output relation for the MIMO channel is:

$$\mathbf{r} = \mathbf{H} \cdot \mathbf{x} + \mathbf{n} \tag{6}$$

where **r** is the array of signals received by the N_R antennas, of size $[N_R, 1]$:

$$\mathbf{r} = \left[r_1, r_2 \ \ldots \ r_{N_R} \right]^T \tag{7}$$

and **H**, of size $[N_R \text{ x } N_T]$, is the channel matrix, also called the transfer function, having the form at moment t:

$$\mathbf{H}_t = \begin{bmatrix} h_{1,1}^t & h_{1,2}^t & \cdots & h_{1,N_T}^t \\ h_{2,1}^t & h_{2,2}^t & \cdots & h_{2,N_T}^t \\ \vdots & \vdots & \ddots & \vdots \\ h_{N_R,1}^t & h_{N_R,2}^t & \cdots & h_{N_R,N_T}^t \end{bmatrix} \tag{8}$$

The $h_{i,j}$ coefficients are actually the channel fading coefficients between the emitting antenna i and the receiving antenna j. These coefficients change in time and are described by various statistical models. For our study, we assume the Rayleigh model for which the fading coefficients are random complex Gaussian variables, with identical distribution with zero mean and unit variance.

n from (6) is the column array of noise (Gaussian or impulsive):

$$\mathbf{n} = \left[\eta_1, \eta_2 \ \ldots \ \eta_{N_R} \right]^T \tag{9}$$

At moment t, the signal received by antenna j will be given by:

$$r_j^t = \sum_{i=1}^{N_T} h_{ji}^t \cdot x_i^t + \eta_j^t, \tag{10}$$

For the specific scheme proposed by Alamouti, there are two emitting antennas and N_R receiving ones. In this paper, we will consider two emitting and two receiving antennas, with BPSK modulation. The advantage of the Alamouti space-time codes consists in developing space-time diversity and decoding [9].

The encoder structure proposed by Alamouti is shown in fig. 1:

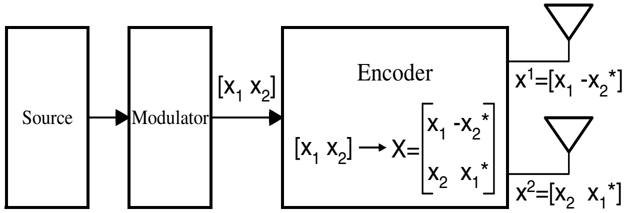

Fig. 1 Alamouti encoder structure

At each coding operation, the group of the two modulated symbols is transmitted according to the following scheme:

$$\begin{array}{c|cc|} & t & t+\tau \\ \hline T_{x1} & x_1 & -x_2^* \\ T_{x2} & x_2 & x_1^* \end{array} \tag{11}$$

At moment t, the first antenna (denoted by T_{x1}) transmits the signal x_1, and the T_{x2} antenna, the signal x_2. At the following moment, $t+\tau$, the signals emitted by the two antennas are $-x_2^*$ and x_1^*, respectively.

At the receiving end, the signals are given by:

$$\begin{cases} r_{j,1} = h_{j,1} \cdot x_1 + h_{j,2} \cdot x_2 + \eta_{j,1} \\ r_{j,2} = -h_{j,1} \cdot x_2^* + h_{j,2} \cdot x_1^* + \eta_{j,2} \end{cases} \tag{12}$$

The matrix form is:

$$\mathbf{r}_j = \begin{bmatrix} r_{j,1} & r_{j,2} \end{bmatrix} = \begin{bmatrix} h_{j,1} & h_{j,2} \end{bmatrix} \begin{bmatrix} x_1 & -x_2^* \\ x_2 & x_1^* \end{bmatrix} + \begin{bmatrix} \eta_{j,1} & \eta_{j,2} \end{bmatrix} \tag{13}$$

The decoding is based on the maximum likelihood algorithm, which selects the most probable symbols $\hat{x}_1$ and $\hat{x}_2$. Considering that the information source is without memory, the modulated symbols x_2 and x_1 are independent from each other. Hence, separate decoding of the two symbols is possible:

$$\hat{\mathbf{x}} = \begin{bmatrix} \hat{x}_1 \\ \hat{x}_2 \end{bmatrix} = \begin{bmatrix} \underset{\hat{x}_1 \in S}{\arg\min} \left(\sum_{j=1}^{N_R} \left| \tilde{r}_{j,1} - \left(\left|h_{j,1}\right|^2 + \left|h_{j,2}\right|^2 \cdot \hat{x}_1 \right) \right|^2 \right) \\ \underset{\hat{x}_2 \in S}{\arg\min} \left(\sum_{j=1}^{N_R} \left| \tilde{r}_{j,2} - \left(\left|h_{j,1}\right|^2 + \left|h_{j,2}\right|^2 \cdot \hat{x}_2 \right) \right|^2 \right) \end{bmatrix}, \tag{14}$$

where

$$\tilde{\mathbf{r}}_j = \begin{bmatrix} \tilde{r}_{j,1} & \tilde{r}_{j,2} \end{bmatrix}^T = \mathbf{H}^H \cdot \mathbf{r}_j^T \tag{15}$$

and $(.)^H$ stands for conjugate transpose of the matrix.

4 Simulation Results

In this section, firstly we analyze the Middleton Class-A impulse noise, for various parameters that describe its statistical model and then we investigate its influence on the Alamouti code performances for two emitting and two receiving antennas.

4.1 Pdf Analysis

For the impulse noise analysis, we considered the model described in [6]. The simulations were done in Matlab for a number of 10^4 samples, by varying the model's *A* and *T* parameters. The Middleton Class-A noise was generated by the InterferenceModeling and Mitigation Toolbox [10]. The values for *A* were considered in the range $[10^{-4}, 1]$, and for *T* in the range $[10^{-2}, 1]$.

Figure 2 shows a comparison between the normal distribution with zero mean and unit variance and the Middleton Class-A model, for different combinations of parameters A=1, 0.1 and T=1, 0.1. We can observe that along with decreasing the impulse index *A*, the AWCN noise's distribution is "narrower" and taller than the Gaussian one and, when T grows, the AWCN distribution approaches the normal one.

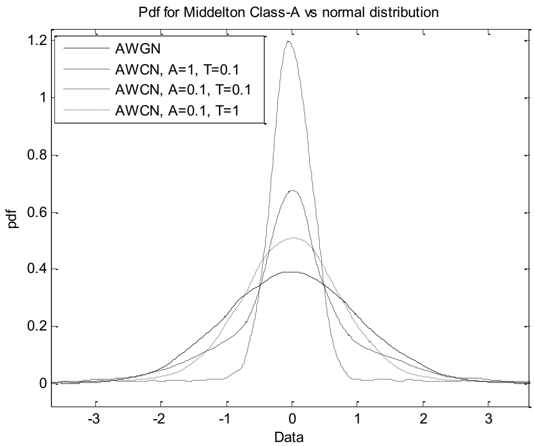

Fig. 2 Middelton Class-A distribution vs normal distribution

For *A*=1 and *T*=1, the two distributions are identical. To emphasize the impulse noise deviation from the normal distribution, we chose the parameters *A*=0.1 and

T=0.1. In Figure 3, this deviation is exemplified with the help of the cumulative density function.

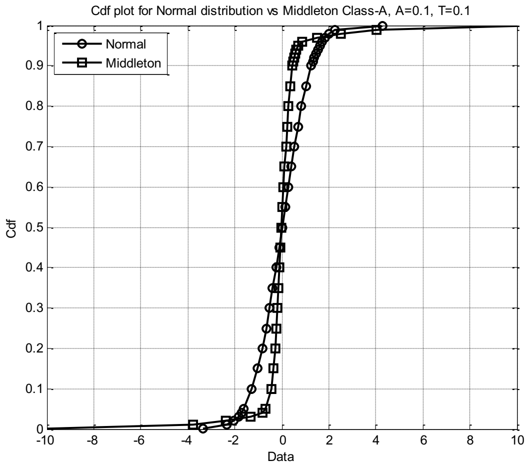

Fig. 3 Middleton Class-A samples distribution vs normal distribution

Figure 4 shows two probability density functions: the real one, obtained by means of generated noise samples and the estimated one, obtained on the base of a normal kernel function, using a window parameter that is a function of the number of points in data samples. The distribution parameters are A=0.1 and T=0.1.

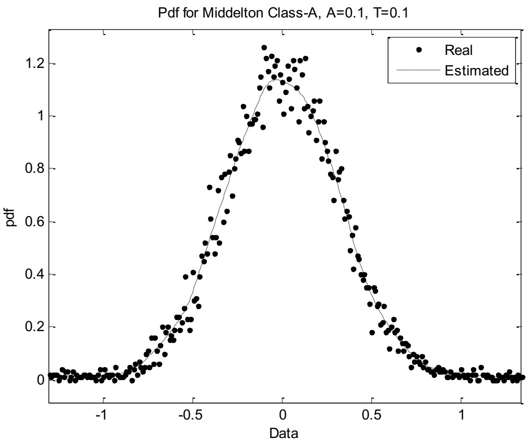

Fig. 4 Pdf for Middelton Class-A, A=0.1, T=0.1

Figure 5 shows the estimated pdfs for the Middleton Class-A noise, for a fixed value T=0.1 of the Gaussian factor and different impulse index values $A \in [10^{-4}, 1]$.

An interesting aspect that can be observed is that for a very small value of A, A=0.0001, the distribution approaches the normal one. This happens because the impulses are very rare or even singular, but with high amplitude, in order to have the same power. Therefore the distribution is practically close to a normal one, the noise being in this case predominantly Gaussian.

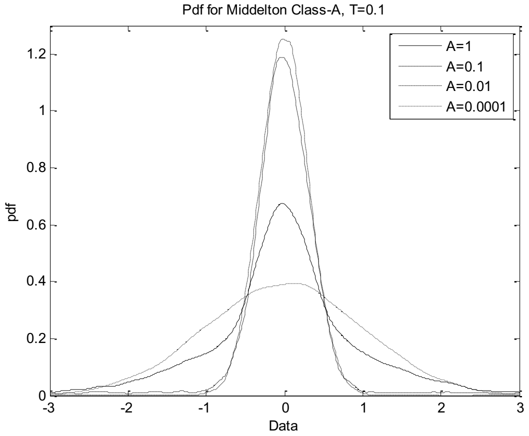

Fig. 5 Estimated pdfs for Middleton Class-A, T=0.1

In Figure 6, the parameter A was fixed at 0.01 and the Gaussian factor T was the one being varied. This influenced the Middleton Class-A distribution by considerably increasing the peak value of the pdf, compared to the normal one.

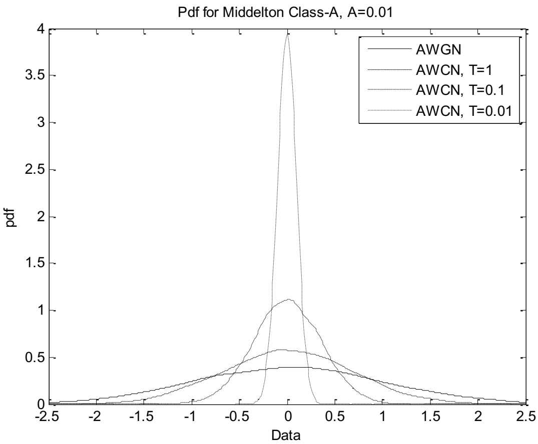

Fig. 6 Estimated pdf for Middleton Class-A, A=0.01

4.2 Bit Error Rate Analysis

Figures 7 and 8 show the Alamouti code performances using the Middleton Class-A type of impulsive noise, with two emitting and two receiving antennas, for a channel affected by Rayleigh fading and BPSK modulation. The code performance is evaluated through the Bit Error Rate (BER) curves, for various values of the parameters *A* and *T*, respectively. The simulations were done for *A*=0.01, 0.1, 1 and *T*=0.01 fixed; and for *T*=0.01, 0.1, 1 and *A*=0.01 fixed, respectively. The analysis is performed by reference to the results in [6] We mention that the performances from [6] of the same Alamouti code, evaluated through the Symbol Error Rate (SER), are given in figure 2, for the QPSK modulations, 16-QAM and for *A*=0.01, 0.1, 1 and *T*=0.01 fixed. Because for a BPSK modulation there is a single bit per symbol, this means that BER and SER are identical. Therefore, we can compare the results we obtained with those from [6] in terms of SER.

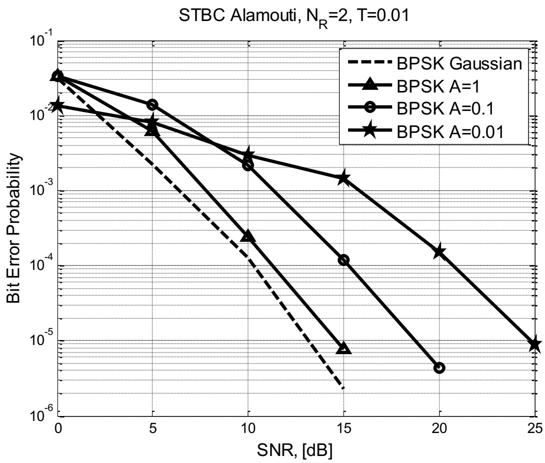

Fig. 7 Performance of Alamouti code, for different impulse index *A* and fixed *T*

For AWGN noise, the Alamouti code ensures an encoding gain of approximately 11dB [11]. Figure 7 shows the fact that, in the presence of impulse noise, the system has weaker performances than in the case of Gaussian noise. Starting from SNR=8dB, once the *A* parameter is lowered, the BER increases, the poorest results being for *A*=0.01. For low SNR values, the system behaves better in the presence of impulsive noise, for *A*=0.01. As the SNR increases, the performances drop significantly for the Middleton Class-A model, with *A*=0.01, compared to AWGN. This happens because, at high SNR values, the impulsive component has a significant influence. Comparing the code performances for different values of *A*, we observe that for high values of *A*, the BER is lower, and for *A*=1, it approaches AWGN.

Unlike the results in [6] for QPSK modulation, we can observe that for SER=10^{-4} and *A*=0.01, in the case of BPSK modulation, an approximately 4dB lower SNR is needed; when *A*=0.1, SNR is smaller with approximately 3 dB, and when A=1, SNR is smaller with approximately 3.5 dB. For AWGN only, the difference between SNRs for QPSK and BPSK is approximately 5 dB. For low SNR values, when A=0.01, the BPSK modulation leads to better performances than QPSK. For example, at SNR=0 dB, in the case of QPSK modulation, SER=3×10^{-2}, compared to the BPSK modulation, when SER=10^{-2}. These performance differences were expected, because the QPSK modulation is more sensitive to noise than the BPSK modulation, the minimum distance between the QPSK constellation points being $\sqrt{2}$, compared to 2 for BPSK.

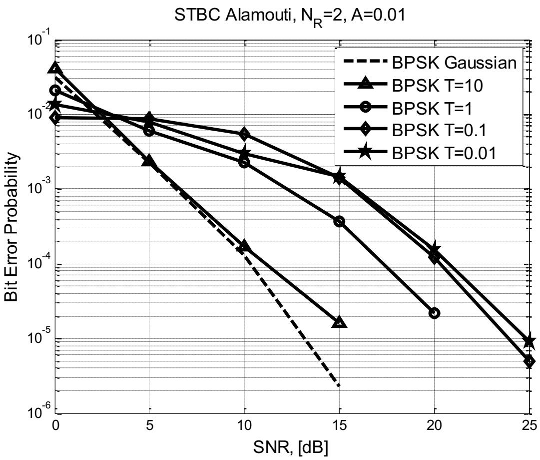

Fig. 8 Performance of Alamouti code, for different T and fixed A

In Figure 8, the parameter A was considered to be constant, at 0.01, and the parameter T was varied, in order to observe its influence on the code's performances. The same conclusion can also be drawn in this case: for SNR values higher than 4dB, when we decrease the Gaussian factor T, the performances drop compared to the AWGN case. For T=1, the BER values are very close to AWGN, and for T=0.1, respectively 0.01, they are different from AWGN, but almost identical to each other. For low SNR values, below 4dB, the opposite occurs: performances slightly increase as T decreases. We cannot anymore compare the obtained results with those in [6], because we have used two receiving antennas, unlike the case addressed in [6], with one receiving antenna.

5 Conclusions

To model the impulsive noise, a Middleton Class-A model was used. A comparative analysis between this type of noise and AWGN was conducted using the probability distributions. The conclusion drawn was that by varying the parameters that describe the model and for lower values of the impulse index and Gaussian factor, the distribution significantly differs from the normal one, except for *A*=0.0001. The influence of the Middleton Class-A noise on the Alamouti code performances was investigated, using two emitting and two receiving antennas, for a channel affected by Rayleigh fading and BPSK modulation. Simulations shown that, for SNR values above 8dB, the performances drop considerably, compared to the Gaussian noise, as the impulse model's parameters get lower. For *A*=1 or above and for *T*>1, the BER values almost reach the ones obtained for the AWGN case. For smaller SNR values, the performances improve in the case of impulsive noise for parameter values as low as possible. The BPSK modulation is more robust than QPSK one, used in transmission over impulse noise environment using an Alamouti code.

References

1. Guey, J.-C., Fitz, M.P., Bell, M.R., Kuo, W.-Y.: Signal design for transmitter diversity wireless communication systems over Rayleigh fading channels. In: Proc. IEEE VTC 1996, pp. 136–140 (1996)
2. Tarokh, V., Seshadri, N., Calderbank, A.R.: Space–time codes for high data rate wireless communication: Performance analysis and code construction. IEEE Transactions on Information Theory 44(2), 744–765 (1998)
3. Middleton, D.: Statistical-physical models of electromagnetic interference. IEEE Trans. Electromagn. Compat. EMC-19(3), 106–127 (1977)
4. Kanemoto, H., Miyamoto, S., Morinaga, N.: Statistical model of microwave oven interference and optimum reception. In: Proc. IEEE ICC 1998, pp. 1660–1664 (October 1998)
5. Win, M., Pinto, P., Shepp, L.: A mathematical theory of network interference and its applications. Proc. IEEE 97(2), 205–230 (2009)
6. Gong, Y., Wang, X., He, R., Pang, F.: Performance of Space-Time Block Coding under Impulsive noise Enviroment. In: Proc. IEEE of 2nd International Conference on Advanced Computer Control, vol. 4, pp. 445–448 (March 2010)
7. Madi, G., Sacuto, F., Vrigenau, B., Agba, B.L., Pousser, Y., Vauzelle, R., Gagnon, F.: Impacts of impulsive noise from partial discharges on wireless systems performance: application to MIMO precoders. EURASIP Journal on Wireless Communications and Networking (2011)
8. Bhatti, S.A., Shan, Q., Glover, I.A., Atkinson, R., Portugues, I.E., Moore, P.J., Rutherford, R.: Impulsive noise modeling and prediction of its impact on the performance of WLAN receiver. In: 17th European Signal Processing Conference (EUSIPCO 2009), pp. 1680–1684 (August 2009)
9. Alamouti, S.M.: A simple transmit diversity technique for wireless communications. IEEE Journal on Selected Areas in Comm 16(8), 1451–1458 (1998)
10. Gulati, K., Nassar, M., Chopra, A., Ben Okafor, N., DeYoung, M., Aghasadeghi, N., Sujeeth, A., Evans, B.L.: InterferenceModeling and Mitigation Toolbox 1.6, for Matlab. ESP Laboratory, ECE Dept., Univ. of Texas at Austin (October 2001)
11. Jafarkani, H.: Space-Time Coding Theory and Practice, p. 58. Cambridge University Press (2005)